JACC: BASIC TO TRANSLATIONAL SCIENCE VOL. 8, NO. 8, 2023

ORIGINAL RESEARCH - PRECLINICAL

Cardiac Lymphatic Insufficiency Leads to Diastolic Dysfunction Via Myocardial Morphologic Change

Zhongyue Pu, MD, PhD,[a] Yuuki Shimizu, MD, PhD,[a] Takumi Hayashi, MD,[a] Yiyang Che, MD,[a] Junya Suzuki, MD,[a] Kazuhito Tsuzuki, MD, PhD,[a] Shingo Narita, MD,[a] Rei Shibata, MD, PhD,[b] John W. Calvert, PhD,[c] Toyoaki Murohara, MD, PhD[a]

VISUAL ABSTRACT

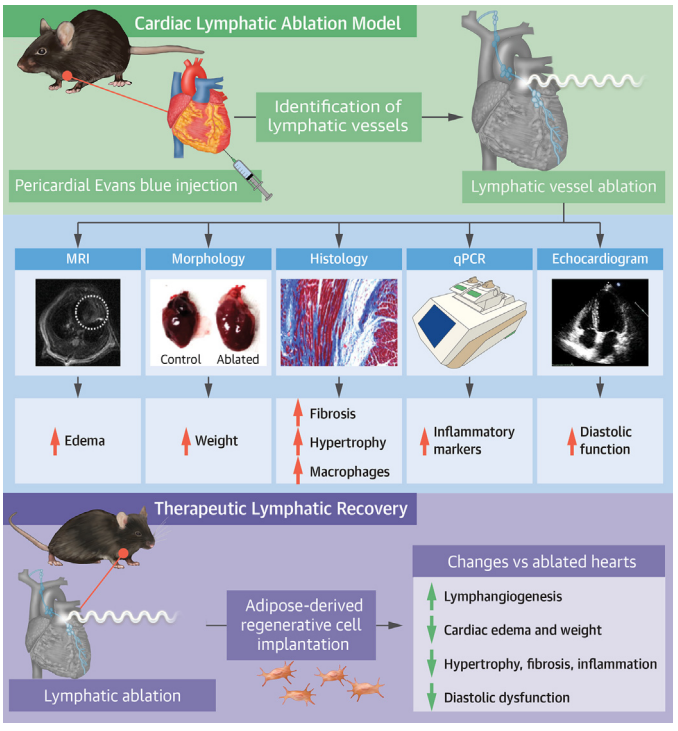

Pu Z, et al. J Am Coll Cardiol Basic Trans Science. 2023;8(8):958-972.

HIGHLIGHTS

- **The authors established a first-ever mouse model of cardiac lymphatic dysfunction in a healthy heart and demonstrated the crucial role of cardiac lymphatic vessels in maintaining cardiac homeostasis and cardiac function both in physiologic and pathologic settings.**
- **Cardiac lymphatic insufficiency itself contributes to the development of myocardial edema, inflammation, and fibrosis, leading to cardiac hypertrophy and resulting in cardiac diastolic dysfunction.**
- **Therapeutic lymphangiogenesis aimed to reconstruct the cardiac lymphatic network could rescue the adverse morphologic changes and heart failure caused by cardiac lymphatic insufficiencies.**

From the [a]Department of Cardiology, Nagoya University Graduate School of Medicine, Nagoya, Japan; [b]Department of Advanced Cardiovascular Therapeutics, Nagoya University Graduate School of Medicine, Nagoya, Japan; and the [c]Carlyle Fraser Heart Center, Division of Cardiothoracic Surgery, Department of Surgery, Emory University School of Medicine, Atlanta, Georgia, USA.
The authors attest they are in compliance with human studies committees and animal welfare regulations of the authors' institutions and Food and Drug Administration guidelines, including patient consent where appropriate. For more information, visit the Author Center.

Manuscript received June 14, 2022; revised manuscript received January 18, 2023, accepted January 18, 2023.

ISSN 2452-302X https://doi.org/10.1016/j.jacbts.2023.01.008

SUMMARY

Although cardiac lymphatic vessels have received increasing attention in recent years, there is still a knowledge gap between cardiac lymphatics and heart homeostasis in a normal heart. In the present study, we established a mouse model of cardiac lymphatic insufficiency ablating cardiac lymphatic collector vessels to reveal the crucial role of cardiac lymphatic vessels in maintaining cardiac homeostasis and the impact on cardiac function both in physiological and pathologic settings. Furthermore, therapeutic lymphangiogenesis improved the adverse effect on cardiac morphologic changes and functions. These findings suggest that the cardiac lymphatic system would be a novel therapeutic target for heart disease. (J Am Coll Cardiol Basic Trans Science 2023;8:958–972)

ABBREVIATIONS AND ACRONYMS

ADRC = adipose-derived regenerative cell

BNP = B-type natriuretic peptide

HFD = high-fat diet

POD = postoperative day

qPCR = quantitative polymerase chain reaction

The main function of lymphatic vessels is to drain extracellular interstitial fluid, which contains proteins, lipids, and immune cells, and return it back to the venous circulation.[1] Therefore, the lymphatic system plays an important role in maintaining the homeostasis of tissue interstitial spaces and in monitoring a local immune system.[1] However, the study of lymphatic vessels has lagged behind that of blood vessels for several reasons: The lumen of lymphatic vessels is collapsed due to low intravascular pressure, making it difficult to visualize; the vascular wall of lymphatic vessels is more fragile than that of blood vessels; and the flowing lymphatic fluid is colorless and transparent, making tissue lymphatic vessels difficult to identify. In the early 2000s, the discovery of specific markers, such as lymphatic vessel endothelial hyaluronan receptor 1 (LYVE1), podoplanin, and prospero-related homeobox 1 (Prox1), made it possible to distinguish lymphatic endothelial cells.[2] Furthermore, technologic advances in the analysis of genetically modified mice with changes in key players in lymphatic biology, such as vascular endothelial growth factor (VEGF) C, vascular endothelial growth factor receptor (VEGFR) 3, hepatocyte growth factor (HGF), and others, led to breakthroughs in the field of lymphatic research.[3,4]

Although lymphatic vessels are known to exist in the heart and form a network similar to blood vessels, the significance of cardiac lymphatic vessels has not received as much attention over the years compared with blood vessels in the heart. Studies using mice lacking the genes for lymphangiogenesis-promoting central players, such as VEGF-C or its major receptor VEGFR-3, have revealed that in these models the lymphatic vessels are disrupted and that these mice showed pericardial effusion and eventual embryonic lethality.[5] In addition, several studies have reported that modulation of cardiac lymphatic vessels showed cardioprotective effects against myocardial infarction and ischemia-reperfusion injury.[6-8] However, the role of lymphatic vessels in the quiescent physiologic context of the heart remains to be fully elucidated.[9]

Accordingly, we examined the effect of cardiac lymphatic ablation on heart homeostasis under physiologic conditions in a newly developed mouse model of cardiac lymphatic vessel disruption. We also investigated the impact of a high-fat diet on the progression of heart disease under the condition of cardiac lymphatic dysfunction.

METHODS

Additional data, analytic methods, and study materials are available from the corresponding author upon reasonable request. An expanded methods section is included in the Supplemental Appendix.

STUDY DESIGN. The study objective was to examine the effect of cardiac lymphatic dysfunction on heart homeostasis under physiologic and pathologic conditions. To mimic a cardiac lymphatic dysfunction, a new mouse model of cardiac lymphatic vessel ablation was created. Also, a high-fat diet (HFD) model (60% of calories from fat) was used to test the effect of a high-fat diet on the progression of heart disease under lymphatic dysfunction. Both cardiac magnetic resonance imaging (MRI)[10] and fluorescein isothiocyanate-dextran experiments[8] were used to assess cardiac edema and lymphatic drainage capacity. Histologic analysis with the use of wheat germ agglutinin, Masson's trichrome, and F4/80 staining were used to examine cardiomyocyte size, fibrosis, and inflammation, respectively. Echocardiography was used to detect cardiac dysfunction.[10,11] For the biological mechanistic study, we used reverse-transcription quantitative polymerase chain reaction (qPCR) and enzyme-linked immunosorbent assay.[12]

All procedures of animal care and use in this study were approved by the Animal Ethics Review Board of the Nagoya University School of Medicine. The study

FIGURE 1 Establishment of a New Murine Cardiac Lymphatic Vessel Ablation Model

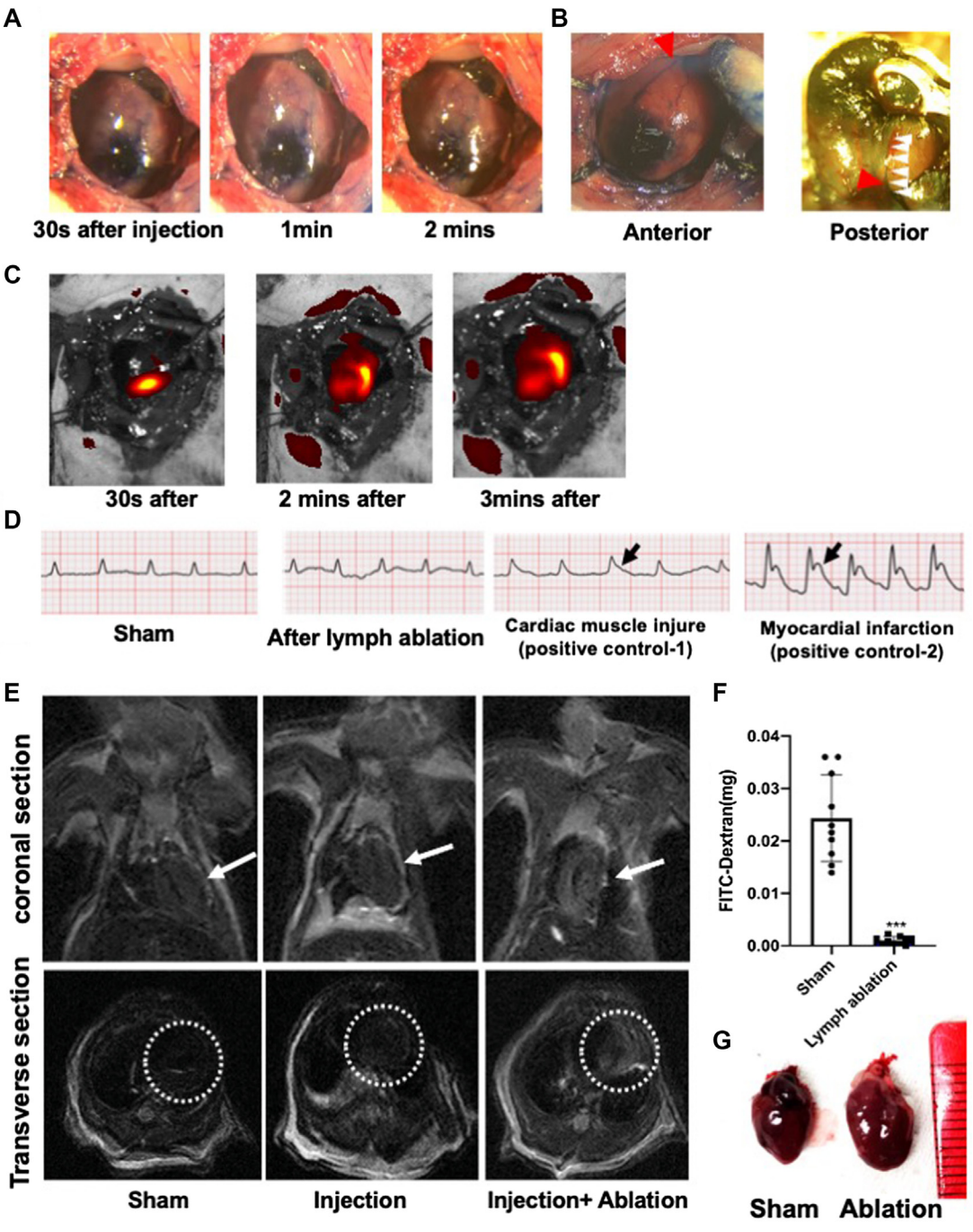

(A and B) Both lymph trunks on the anterior and posterior side of the heart were ablated on the proximal side, indicated by **red arrowheads**, after the Evans blue dye injection. **(C)** Fluorescein isothiocyanate (FITC)–dextran was injected into the apex side of heart to detect the path of lymph drainage as recorded by an in vivo imaging system. **(D)** An electrocardiogram was obtained immediately after lymphatic ablation to determine if lymphatic ablation resulted in ST-segment elevation. **(E)** T2-weighted magnetic resonance imaging was used to assess tissue edema. **(F)** An assessment of the levels of circulating FITC-dextran. Data are presented as mean ± SD (n = 5). ***$P < 0.001$ vs sham; unpaired Student's *t*-test was used to evaluate statistical significance between 2 groups. **(G)** Representative images of the heart 6 weeks after lymph ablation.

conformed to the guidelines from Directive 2010/63/EU of the European Parliament on the protection of animals used for scientific purposes or the National Institutes of Health Guide for the Care and Use of Laboratory Animals. To ensure reproducibility, the mice were assigned randomly to the various experimental groups. The investigators were not blinded to the conduct of the experiment but were blinded to an assessment of outcomes.

All experiments were repeated 3 times independently. The sample sizes (5 to 10) used in each group were predetermined by power analysis. All the details are given in the figure legends along with details of the statistical analysis.

MOUSE MODEL OF CARDIAC LYMPHATIC DYSFUNCTION. To mimic a cardiac lymphatic dysfunction, a new mouse model of cardiac lymphatic vessel ablation was designed. Male C57BL/6J mice (aged 8to10 weeks) were purchased from Charles River Laboratories Japan. Sex influences the development of cardiovascular disease.[13] Therefore, we used only male mice in our studies. This allowed for the evaluation of the impact of cardiac lymph ablation on cardiac homeostasis in a well-controlled experimental system. All the mice were anesthetized with hydrochloric acid medetomidine (0.3 mg/kg), midazolam (4 mg/kg), and butorphanol tartrate (5 mg/kg) before the surgical procedure.[14] Respiration was controlled with a mechanical respirator. A left thoracotomy incision was used to expose the heart. Five microliters of Evans blue dye was injected intramuscularly into the apex side of a beating heart through a 30-gauge needle. After observation for 3 to 5 minutes after injection, the dye was easily followed as it ascended to 2 lymphatic collective vessels before merging into 1 large trunk under the atrium separately on the anterior side. Another lymphatic collective vessel was detected on the posterior side of the heart. Both main lymphatic trunks were ablated by a monopolar radiofrequency electrosurgical instrument.[15] An electrocardiogram was performed immediately after lymphatic ablation to check for ST-segment elevation. The chest was then closed with sutures.

HFD-INDUCED CARDIOMYOPATHY MODEL. The impact of lymphatic dysfunction on the progression of heart disease was also tested in a 60% fat diet model. HFD-induced cardiomyopathy is a well-established model to induce myocardial morphologic changes and cardiac dysfunction.[16] Some mice (L+H group) were started on HFD at the beginning of the lymphatic ablation for 6 weeks and assessed for the following parameters.

CARDIAC LYMPHANGIOGENESIS FOLLOWING TREATMENT WITH ADIPOSE-DERIVED REGENERATIVE CELLS. Adipose-derived regenerative cells (ADRCs) were reported to augment lymphangiogenesis in pathological conditions.[10,15] We therefore used ADRC implantation to reconstruct a lymphatic network and recover cardiac lymphatic function in this study. ADRCs were isolated from the inguinal subcutaneous adipose tissue as described previously.[15] A subset of mice was subjected to cardiac lymphatic ablation and administered an intramyocardial injection of ADRC cells (5×10^5 ADRCs in 10 μL phosphate-buffered saline solution) just after ablation into 3 points of the surgery zones (3 to 5 μL in each site) with a 30-gauge needle. After 6 weeks, mice were killed to evaluate lymphatic capillary density by means of immunofluorescence staining of frozen sections.

LYMPHATIC FUNCTIONAL ASSESSMENT WITH THE USE OF FLUORESCEIN ISOTHIOCYANATE–DEXTRAN AND CARDIAC MRI. We used both invasive and noninvasive techniques to evaluate cardiac lymphatic vessel function with or without ablation of the cardiac lymphatics. Ten microliters of fluorescent dextran molecular probe (fluorescein isothiocyanate–dextran, 2,000 kDa, 2 mg/mL; Thermo Fisher Scientific) was injected intramuscularly into the apex of the heart.[8] Because of its size, the probe was taken up by the lymphatics and then the probe was traced and recorded by an in vivo imaging system (IVIS, Summit Pharmaceuticals International Corp) Blood samples were collected 30 minutes after surgery. To assess how much of the labeled dextran had moved through the cardiac lymphatics into the blood circulation, the fluorescence intensity was detected with a plate reader.[8] A standard curve of the fluorescein isothiocyanate–dextran concentration was made to calculate the amount of the probes in each blood sample. Cardiac edema was examined noninvasively with the use of a 1.5-T whole-body MRI scanner (MRS 3000 Benchtop Magnetic Resonance Imaging Systems, MR Solutions) to produce a T2-weighted image 30 minutes after injecting 5 μL of Evan's blue.[10] We performed radiofrequency calibration once and took images, so that the same hue displays a signal of the same intensity.

CARDIAC FUNCTIONAL ASSESSMENT. Noninvasive echocardiography was performed in sedated[17] mice 6 weeks after surgery. Mice were assessed for both cardiac systolic function and diastolic function with the use of B-mode, M-mode, PW-mode, and tissue Doppler (Vevo 1100 imaging system, Fujifilm Visual Sonics).

FIGURE 2 Morphologic Changes of Myocardium Size, Cardiac Fibrosis, and Cardiac Hypertrophy Under Chronic Lymphatic Dysfunction

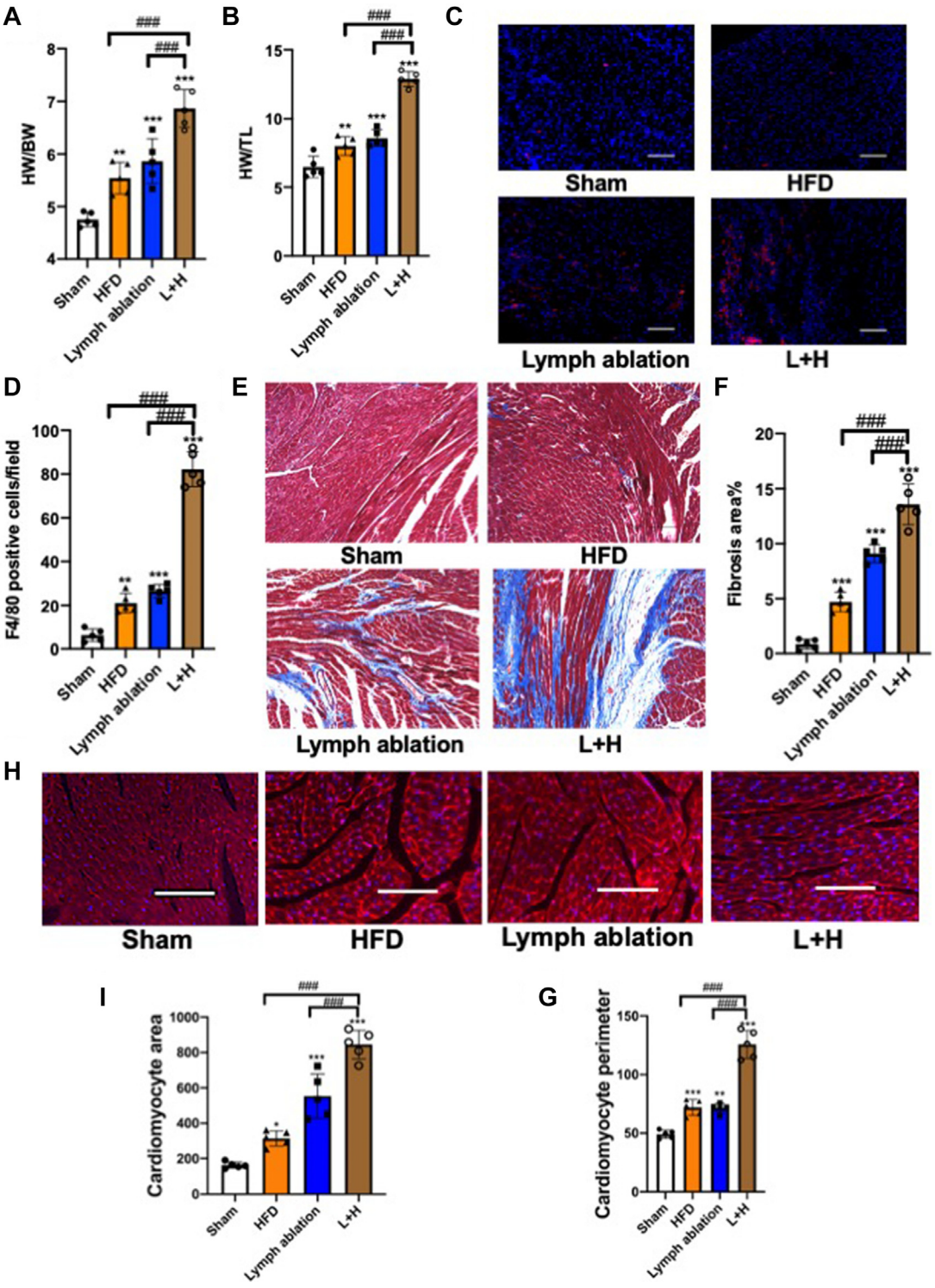

(A and B) Heart weight to body weight (HW/BW) and heart weight to tibia length (HW/TL) ratios. **(C)** Frozen sections were immunostained with anti-F4/80 **(red)** to detect macrophages. Magnification ×20. Scale bar 100 μm. **(D)** Quantitative analysis of the number of macrophages per field. **(E)** Masson's trichrome staining **(blue)** of heart paraffin sections. Magnification ×20. Scale bar 100 μm. **(F)** The percentage of fibrosis area per field. **(H)** Wheat germ agglutinin staining **(red)**. 6-Diamidino-2-phenylindole–stained nuclei are shown in **blue**. Magnification ×20. Scale bar 100 μm. **(I and G)** Quantification of cardiomyocyte cross-sectional area and perimeter. Data are presented as mean ± SEM (n = 5). $^{*}P < 0.05$; $^{**}P < 0.01$; $^{***}P < 0.001$ vs sham, $^{\#\#\#}P < 0.001$ vs L+H; 1-way ANOVA and Tukey post hoc tests. HFD = high-fat diet; L+H = lymphatic ablation plus high-fat diet.

IMMUNOHISTOCHEMISTRY. Tissue samples were collected from mouse hearts in each group and embedded in optimal cutting temperature compound. Frozen sections (6 μm thick) were fixed with 4% paraformaldehyde and then blocked with the use of 1% bovine serum albumin at 25 °C for 1 hour. A primary antibody to LYVE-1 (4:1,000; Acris) was incubated with the sections at 4 °C overnight, followed by incubation with secondary antibodies (Alexa-Fluor 488-conjugated antirabbit antibody, 1:1,000; Thermo Fisher Scientific) at 25 °C for 1 hour.[14,18] The nuclei were stained with 4% 4,6-diamidino-2-phenylindole (1:1,000; Roche). Macrophages were detected by PE antimouse F4/80 mAb (1:1,000; BioLegend).[10] For detection of the size of cardiomyocytes, the sections were incubated with Alexa Fluor 594–conjugate of wheat germ agglutinin (5:1,000; Thermo Fisher Scientific) for 1 hour.[11]

MASSON'S TRICHROME STAINING FOR COLLAGEN VISUALIZATION. Samples were fixed in 4% paraformaldehyde and embedded in paraffin. Sections were sequentially incubated in the following solutions: Bouin's solution (Sigma) (overnight), Weigert's iron hematoxylin working solution (5 minutes), Biebrich scarlet acid solution (2 minutes), phosphomolybdic-phosphotungstic acid solution (5 minutes), aniline blue solution (10 minutes), and 1% acetic acid (Sigma) (2 minutes). Between each solution, the sections were briefly washed with water, and then briefly rinsed in an ascending isopropanol series followed by xylol before a coverslip was added.[11] Images were visualized on a BZ-X710 fluorescence microscope (Keyence) at ×20 magnification, and 5 fields were randomly selected from each slide. We determined the average number of positive cells per field with the use of the Image J software (version 1.51).

REAL-TIME REVERSE-TRANSCRIPTASE pPCR ANALYSIS. Total RNA was extracted with the use of the RNeasy Mini Kit (Qiagen) from mouse cardiac tissue. Reverse transcription was performed using a qPCR RT master mix kit (Toyobo). Real-time reverse-transcription PCR analysis was performed on a C1000 Thermal Cycler (Bio-Rad) using Sybr Green I and the following conditions: 95 °C for 10 minutes followed by 40 cycles at 95 °C for 15 seconds and 60 °C for 45 seconds. The expression of target mRNAs was normalized to that of GAPDH in each sample. The primer sequences (tumor necrosis factor [TNF]-α, interleukin [IL]-1β, IL-6, collagen type I, alpha 1 [COL1A1], transforming growth factor [TGF]-β, periostin [Postn], β-myosin heavy chain (MHC), cation channel subfamily C member 6 [TRPC6], regulator of calcineurin [RCAN] 1, cardiotropin [CT] 1, VEGF-C, VEGF-D, adrenomedullin, VEGFR3, podoplanin, and GAPDH) are listed in the Supplemental Methods.[10]

ENZYME-LINKED IMMUNOSORBENT ASSAY. Plasma was prepared from the blood by centrifugation at 4,000*g* for 10 minutes at 4 °C. Plasma levels of B-type natriuretic peptide (BNP) were measured with the use of the mouse/Rat BNP Enzyme Immunoassay ELISA Kit (RayBiotech) according to the manufacturer's protocols.[14]

STATISTICS. The sample sizes in each group were predetermined by power analysis. The results were expressed as mean ± SD or mean ± SEM. A paired or unpaired Student's *t*-test was used to evaluate statistical significance between 2 groups; 1-way analysis of variance along with Tukey post hoc test for multiple pairwise comparisons was used for 3 or more groups.[10] The normality of all data was verified with the use of the Shapiro-Wilk test.[10] Data were also tested for equal variance by means of the Brown-Forsythe test.[10] All statistical analyses were performed with the use of GraphPad Prism software version 8 (GraphPad Software). A P value <0.05 denoted statistical significance.

RESULTS

ESTABLISHMENT OF A NEW MOUSE MODEL OF CARDIAC LYMPHATIC DYSFUNCTION. Figure 1A shows cardiac lymphatic fluid drainage following the intramuscular injection of Evans blue dye into the apex of the heart. Over 3 to 5 minutes the Evans blue dye ascended to 2 lymphatic collecting vessels that merge into 1 large trunk under the atrium separately on the anterior side (Figure 1B, left). Another lymphatic collective vessel was detected on the posterior side of the heart (Figure 1B, right). IVIS analysis also showed that an injection of fluorescein isothiocyanate-dextran into the apex site was drained in a similar manner (Figure 1C). Both sides of the cardiac collective lymphatic vessels were ablated at the site indicated by the red arrows in Figure 1B. Figure 1D shows that lymphatic ablation did not induce acute cardiac injury, as assessed with electrocardiography. For comparison, we show ST-segment elevations resulting from a murine cardiac muscle injury model and a myocardial infarction model. After ablation of cardiac lymphatic vessels, lymphatic fluid accumulated in the heart, as shown by a high-intensity area in the T2 MRI image (Figure 1E). In terms of a functional assessment, the lymphatic drainage capacity of heart tissue was reduced after the lymphatic ablation

FIGURE 3 Cardiac Inflammation, Fibrosis, and Hypertrophic Signaling After Cardiac Lymphatic Ablation

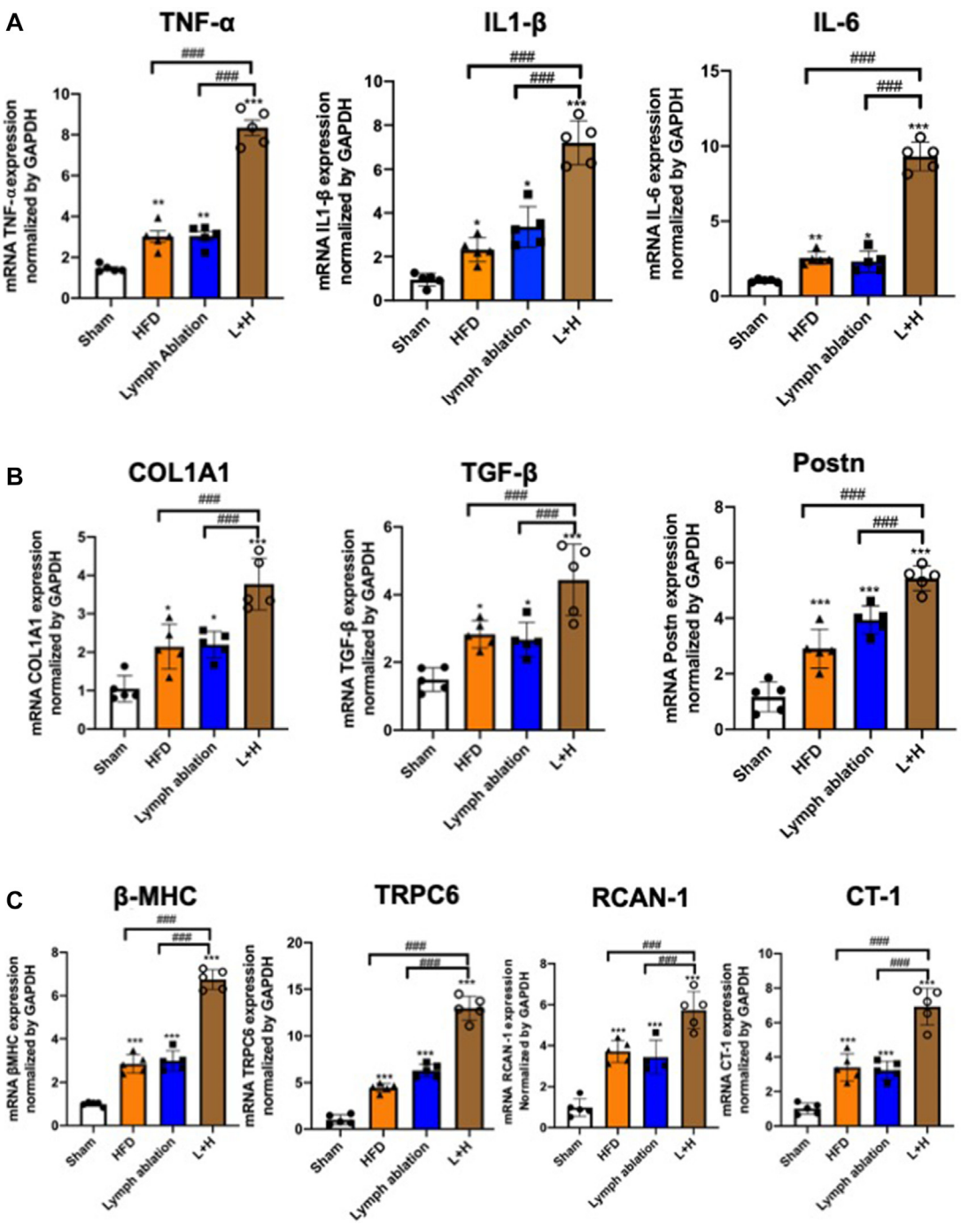

(A) The mRNA expression levels of tumor necrosis factor (TNF)-α, interleukin (IL)-1β, and IL-6 were assessed in the myocardium of sham-operated (sham), HFD, lymph ablation, and L+H mice 6 weeks after surgery. **(B)** The mRNA expression levels of fibrosis mediation factors collagen type I, alpha 1 (COL1A1), transforming growth factor (TGF) β, and periostin (Postn) increased after cardiac lymph ablation. **(C)** The mRNA expression levels of sensitive markers of pathologic hypertrophy β-myosin heavy chain (MHC), transient receptor potential cation channel subfamily C member 6 (TRPC6), regulator of calcineurin (RCAN) 1, and cardiotropin (CT) 1,were increased after cardiac lymph ablation. Data are presented as mean ± SEM (n = 5). $^{*}P < 0.05$; $^{**}P < 0.01$; $^{***}P < 0.001$ vs sham; $^{\#\#\#}P < 0.001$ vs L+H; 1-way ANOVA and Tukey post hoc tests. Abbreviations as in Figure 1.

(Figure 1F). In addition, ablation of cardiac lymphatics induced an increase in the size of the heart compared with sham-operated hearts at postoperative day (POD) 42 (Figure 1G). Heart weight was increased after cardiac lymphatics ablation compared with the sham group at POD 42 (Figures 2A and 2B). Furthermore, although the HFD-induced cardiomyopathy model displayed heavier heart weight, we found cardiac lymphatics ablation deteriorates those responses in this model (Figures 2A and 2B).

LYMPHATIC VESSEL ABLATION INDUCES REACTIONS IN THE HEART. Histologic analysis demonstrated that cardiac lymphatic ablation induced macrophage accumulation in the myocardium (Figure 2C and 2D). In addition, cardiac fibrosis was induced at POD 42 after lymphatics ablation (Figures 2E and 2F). Cardiomyocytes also displayed hypertrophy as evidenced by an increase in cross-sectional area and perimeter (Figures 2G and 2H). These changes were all augmented when lymphatic ablation was combined with HFD-induced obesity.

HFD COMBINED WITH LYMPHATIC DYSFUNCTION AUGMENTS THE REACTIONS IN THE HEART. Given that excessive inflammation is one of the factors for tissue edema, which could also induce fibrosis, we next evaluated the expression of inflammatory and profibrotic signaling markers in the heart.

qPCR showed that the expressions of inflammatory factors, such as tumor necrosis factor (TNF)-α, interleukin (IL)-1β, and IL-6, were up-regulated in the lymphatic ablation group at POD 42 after injury (TNF-α 2.08-fold, IL-1β 3.55-fold, and IL-6 2.26-fold) (Figure 3A). Figure 3B shows that the expressions of profibrotic factors, such as COL1A1, TGF-β, and Postn, were up-regulated in the lymphatic ablation group (COL1A1 2.09-fold, TGF-β 1.79-fold, and Postn 3.36-fold). We subsequently examined the expression of β-MHC, TRPC6, RCAN-1, and CT-1, molecules relating to hypertrophy in cardiomyocytes. Figure 3C shows that the expression of β-MHC, TRPC6, RCAN-1, and CT-1 was up-regulated in the lymphatic ablation group (β-MHC 3.03-fold, TRPC6 6.29-fold, RCAN-1 3.53-fold, and CT-1 3.22-fold higher than in the sham group). Again, these changes were all augmented when lymphatic ablation was combined with HFD-induced obesity.

CARDIAC LYMPHATIC DYSFUNCTION LEADS TO CARDIAC DIASTOLIC DYSFUNCTION. To test whether the observed histologic changes induced by lymphatic ablation could affect cardiac function, we assessed both systolic function and diastolic function by echocardiography. Figure 4A shows representative M-mode images in each group at POD 42. Although systolic functions in terms of left ventricular ejection fraction showed no changes between each group, wall thickness increased in the lymphatic ablation group (Figures 4B to 4E). In contrast, diastolic function as evaluated by E/A and E/e′ were both reduced in the lymphatic ablation group. Furthermore, the L+H group displayed an augmented increase in wall thickness and remarkable diastolic dysfunction at POD 42 compared with the HFD group or the lymphatic ablation group (Figures 4F to 4I).

IMPLANTATION OF ADRCs ATTENUATES CARDIAC HYPERTROPHY VIA PROMOTING LYMPHANGIOGENESIS. Because ADRCs promote lymphangiogenesis in multiple damaged tissues,[10,15] we next tested whether the improvement of cardiac lymphatic function by implantation of ADRCs could lead to the suppression of cardiac hypertrophy in this model. Supplemental Figure 1 shows that ADRC implantation promoted lymphangiogenic growth factors expression in the edematous heart. Histologic analysis demonstrated that the lymphatic rarefaction observed in the L+H group was attenuated by ADRC implantation (Figures 5A and 5B), which was also confirmed with the augmentation of the expressions of VEGFR3 and podoplanin according to qPCR (Supplemental Figure 2A). ADRCs reduced the dilation of lymphatic lumens (a marker of lymphatic fluid congestion) and induced lymphangiogenesis (Figure 5C). Supplemental Figure 3A shows that the wet and dry ratio (Supplemental Methods) of the heart was increased with cardiac lymphatic ablation, which was attenuated by therapeutic lymphangiogenesis with ADRC, resulting in reducing cardiac high-intensity signal in T2-weighted MRI after cardiac lymphatic ablation (Supplemental Figure 3B). Furthermore, the augmentation of lymphangiogenesis by ADRCs ameliorated cardiac lymphatic dysfunction–induced cardiac hypertrophy (Figures 5D to 5F), reduced macrophage accumulation (Figures 5G and 5H), and attenuated fibrosis (Figures 5I and 5J). Finally, cardiomyocytes displayed less hypertrophy in the ADRC implantation group (Figures 5K and 5L).

CARDIAC LYMPHANGIOGENESIS INDUCED BY ADRCs AMELIORATES THE PATHOLOGIC RESPONSES. Figure 6A shows that the inflammatory reactions (as measured by TNF-α, IL-1β, and IL-6 expression) in the heart were significantly up-regulated in response to cardiac lymphatic injury. Conversely, the expressions of those markers were improved by augmentation of lymphangiogenesis by ADRC implantation. The up-

FIGURE 4 Cardiac Lymphatic Ablation Induced Cardiac Diastolic Function Impairments in Murine Models

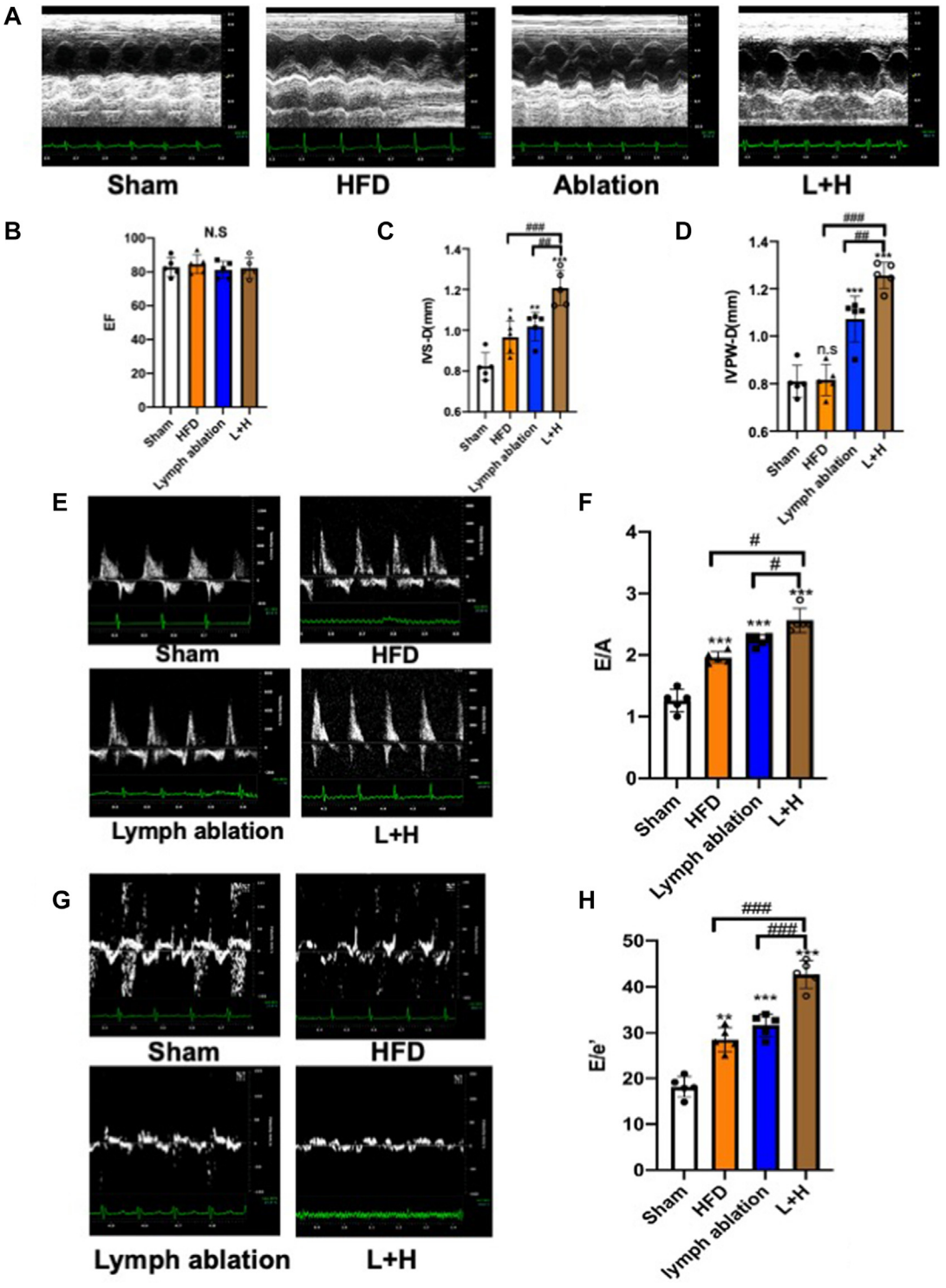

(A and B) Six weeks after surgery, there were no significant differences in left ventricular ejection fraction (EF). **(C and D)** The diastolic interventricular septum thickness (IVS-D) and diastolic left ventricular posterior wall thickness (LVPW-D) were increased by cardiac lymph ablation. **(E and G)** Doppler (E/A ratio) and tissue Doppler (e′ velocity) profiles for the assessment of left ventricular diastolic function for the 4 groups 6 weeks after surgery **(F)** Ratio of flow Doppler E-wave to A-wave amplitude. **(H)** Ratio of flow Doppler E-wave amplitude to tissue Doppler E′-wave amplitude. Data are presented as mean ± SEM (n = 5). $^{**}P < 0.01$; $^{***}P < 0.001$ vs sham; $^{\#}P < 0.05$; $^{\#\#\#}P < 0.001$ vs L+H; 1-way ANOVA and Tukey post hoc tests. Abbreviations as in Figure 1.

regulation of profibrotic factors by cardiac lymphatic ablation, such as COL1A1, TGF-β, and Postn, was also suppressed by augmentation of lymphangiogenesis in the L+H+ADRC group (**Figure 6B**). In addition, cardiac hypertrophic signaling induced by cardiac dysfunction, measured by the expression of markers such as β-MHC, TRPC6, RCAN-1, and CT-1, was ameliorated by the augmentation of lymphangiogenesis (**Figure 6C**). Taken together, cardiac lymphatic dysfunction promoted inflammation, fibrotic formation, and cardiac hypertrophy, and therapeutic lymphangiogenesis suppressed these effects.

THERAPEUTIC LYMPHANGIOGENESIS DEMONSTRATES A CARDIOPROTECTIVE EFFECT ON DIASTOLIC DYSFUNCTION. Finally, we tested whether cardiac lymphatic dysfunction-induced cardiac diastolic dysfunction could be improved by therapeutic lymphangiogenesis. As shown in **Figures 7A and 7B**, systolic function demonstrated no remarkable change, regardless of the change in cardiac lymphatics function at POD 42 in this model. In contrast, wall thickness displayed hypertrophic changes in the L+H group, which was reduced by recovery of cardiac lymphatic functions with ADRC implantation (**Figure 7C**). Although the plasma BNP level increased in response to cardiac lymphatic ablation at POD 42, therapeutic lymphangiogenesis decreased the expression of this biomarker of heart failure (**Figure 7D**). In addition, **Figures 7D to 7G** show that diastolic function evaluated according to E/A and E/e′ was reduced under cardiac lymphatic dysfunction, and this effect could be suppressed by therapeutic lymphangiogenesis.

DISCUSSION

Because of limitations regarding the visualization and assessment of cardiac lymphatic vessels, research on the cardiac lymphatic system has received very little attention in the past decade. However, the importance of this little-understood system has come into the limelight in recent years, resulting in a burst of studies.[19-21] These studies have demonstrated that the cardiac lymphatic network plays an important role in the regulation of myocardial extracellular fluid volume and cardiac immune cell homeostasis, mainly in the setting of pathologic heart conditions.[9,22] For example, cardiac lymphatic vessels undergo rarefaction and/or significant remodeling in various pathologic conditions, resulting in the loss of lymphatic drainage function and the development of tissue edema.[6,23] In addition, clinical studies have reported that patients with myocardial infarction and chronic heart failure show marked remodeling of cardiac lymphatics.[24-26] These findings suggest the pivotal role of the lymphatic system in the development of cardiac diseases, yet little is known about whether a disruption of cardiac lymphatics can induce severe consequences in a quiescent physiologic condition. We think that it is very important to know how cardiac homeostasis is regulated by normal cardiac lymphatic vessels. In the present study, we established a new mouse cardiac lymphatic dysfunction model by ablating precollective lymphatic vessels and tested the impact of cardiac lymphatic dysfunction on heart homeostasis.

Until recently, the lymphatic system has been disregarded when considering patients with heart failure with reduced ejection fraction.[22] However, lymphatic congestion, similarly to venous congestion, is a hallmark of heart failure, and drives both the manifestation of symptoms and adverse outcomes. For example, increased central venous pressure suppressed lymphatic drainage, thereby increasing fluid retention in the cardiac interstitial space. In addition, high tissue pressure results in the impairment of lymphatic vessel integrity and increased vascular permeability.[27] Notably, a 3.5% increase in myocardial fluids may lead to an approximately 30% to 40% reduction in cardiac output.[27,28] Several studies have shown that myocardial edema induced by selective experimental obstruction of cardiac lymphatics rapidly leads to cardiac systolic dysfunction in dogs.[29,30] In addition, Wang et al[31] showed that ligation of the large lymphatic vessels together with resection of the large cardiac lymph nodes resulted in severe myocardial edema and fibrosis within the first 4 weeks after ligation in a rabbit model. However, the degree of lymphatic obstruction and the direct relationship with cardiac diastolic function remained unknown. The present study demonstrates for the first time that both myocardial edema and fibrosis can be induced by lymphatic vessel ablation, resulting in cardiac diastolic dysfunction without remarkable systolic dysfunction at 6 weeks after surgery in a mouse model.

Lymphatic dysfunction and remodeling occur in experimental models of multiple heart failure with preserved ejection fraction (HFpEF)-associated comorbidities.[32-34] For example, diet-induced obesity models showed reduced dermal lymphatic collecting vessel pumping rates, as well as reduced lymphatic capillary density with an accumulation of

FIGURE 5 Cardiac Lymphangiogenesis Caused by ADRC Implantation Improved Cardiac Inflammation, Fibrosis, and Hypertrophy

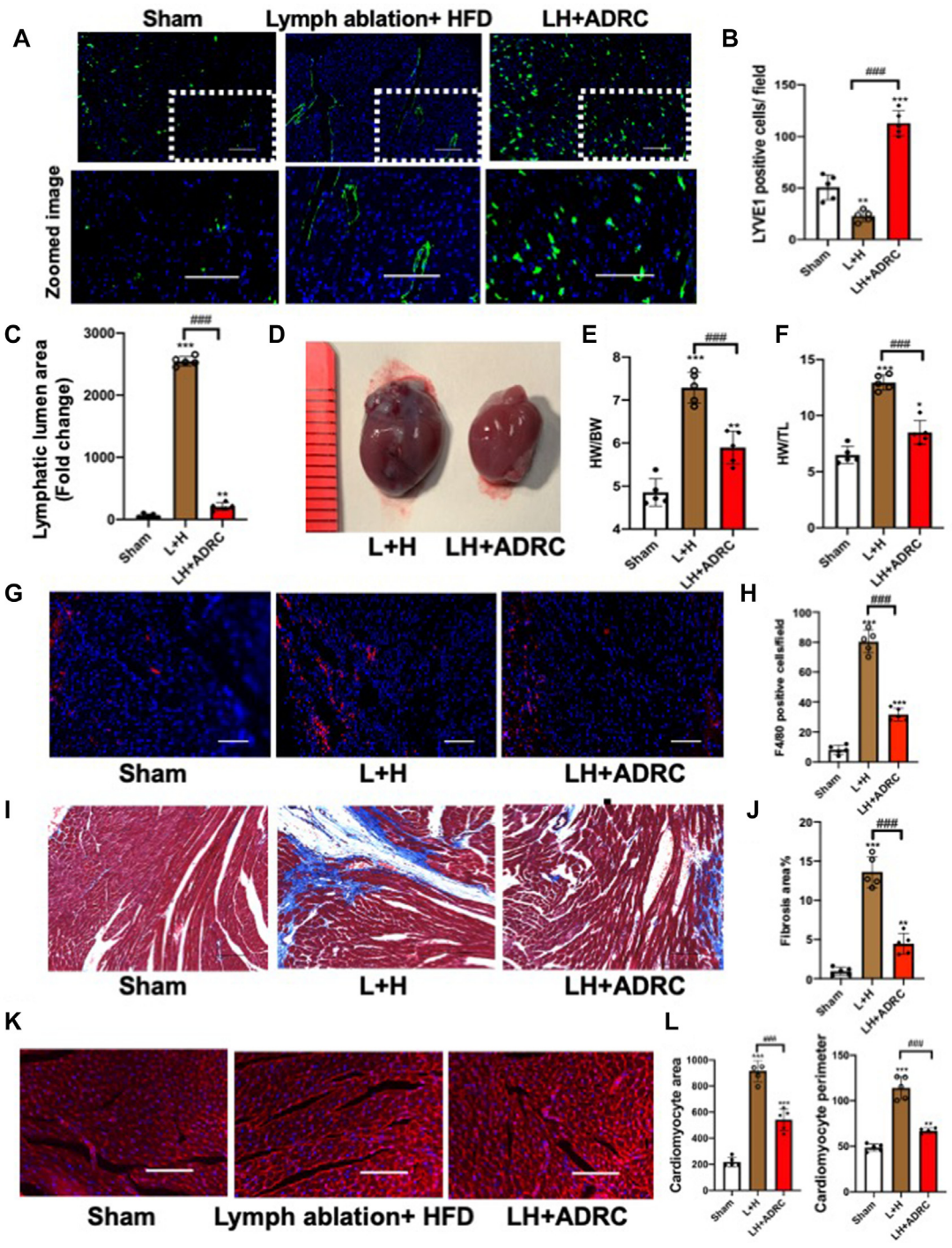

(A) Immunostaining with anti-lymphatic vessel endothelial hyaluronan receptor 1 (LYVE1) **(green)** and 4,6-diamidino-2-phenylindole **(blue)**. Scale bar 100 μm. **(B)** Quantitative analysis of the LYVE1-positive cells. **(C)** Quantification of lymphatic area. **(D)** Representative images of the heart 6 weeks after ADRC implantation. **(E and F)** Heart weight to body weight (HW/BW) and heart weight to tibia length (HW/TL) ratios in the 3 groups. **(G)** Immunostaining with anti-F4/80 **(red)**. **(H)** Quantitative analysis of the number of macrophages per field. **(I)** Masson's trichrome staining **(blue)** of heart paraffin sections. **(J)** The percentage of fibrosis area per field. **(K)** Representative images of wheat germ agglutinin staining **(red)**. **(L)** Quantification of cardiomyocyte cross-sectional area and perimeter. Data are presented as mean ± SEM (n = 5). $^{**}P < 0.01$; $^{***}P < 0.001$ vs sham; $^{\#\#\#}P < 0.001$ vs L+H; 1-way ANOVA and Tukey post hoc tests. Abbreviations as Figure 1.

FIGURE 6 **Expression of Cardiac Inflammatory, Fibrotic, and Hypertrophic Markers Was Decreased by ADRC-Induced Cardiac Lymphangiogenesis**

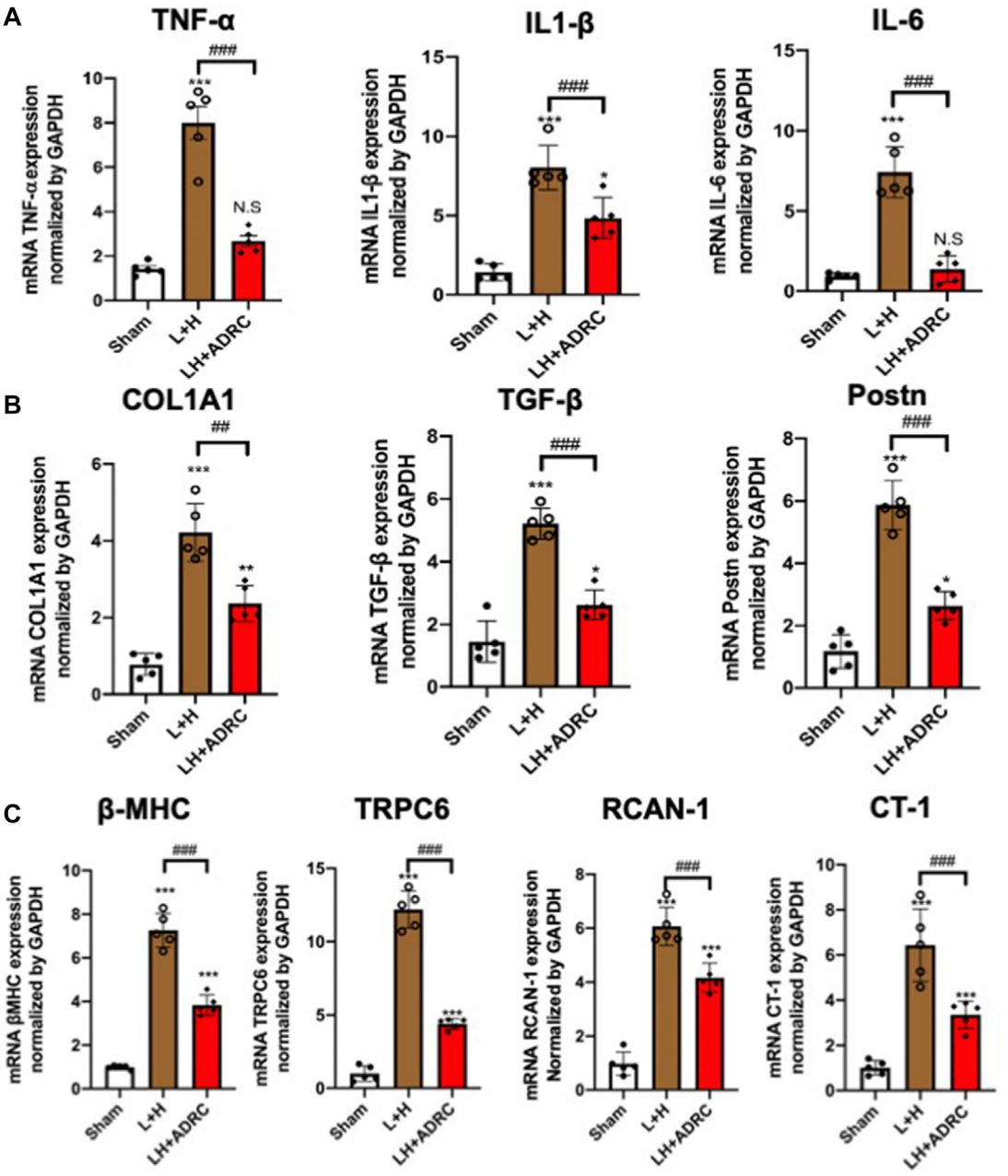

(A) The mRNA expression levels of TNF-α, IL-1β, and IL-6 were assessed in the myocardium of sham-operated, L+H, and L+H+ADRC implantation groups after 6 weeks **(B)** The mRNA expression levels of fibrosis mediation factors COL1A1, TGF-β, and Postn. **(C)** The mRNA expression levels of sensitive markers of pathologic hypertrophy, namely β-MHC, TRPC6, RCAN-1, and CT-1, were decreased in the ADRC implantation group. Data are presented as mean ± SEM (n = 5). *P <0.05; **P <0.01; ***P <0.001 vs sham; $^{\#\#\#}P$ < 0.001 vs L+H; 1-way ANOVA and Tukey post hoc tests. Abbreviations as in Figures 1, 3, and 5.

FIGURE 7 ADRC Implantation Improved Cardiac Diastolic Function Through Cardiac Lymphangiogenesis

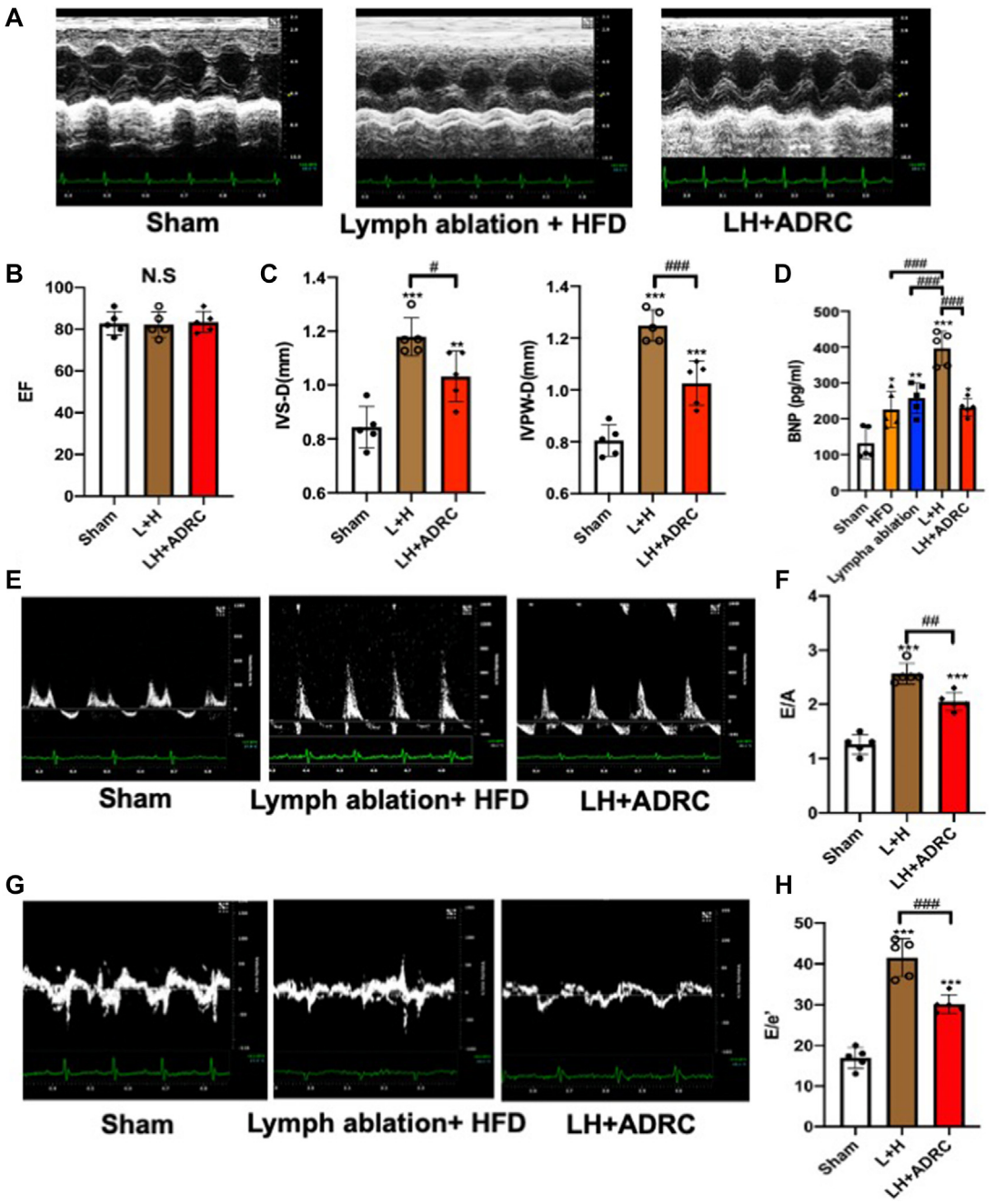

(A and B) There were no significant differences in ejection fraction (EF). **(C)** The IVS-D and LVPW-D trends. **(D)** Circulating B-type natriuretic peptide (BNP) levels detected by enzyme-linked immunosorbent assay were improved after ADRC treatment. **(E and G)** Doppler (E/A ratio) and tissue Doppler (e′ velocity) profiles for the assessment of left ventricular diastolic function for the 4 groups 6 weeks after surgery **(F)** Ratio of flow Doppler E-wave to A-wave amplitude. **(H)** Ratio of flow Doppler E-wave amplitude to tissue Doppler E′-wave amplitude. Data are presented as mean ± SEM (n = 5). $^{***}P < 0.001$ vs sham; $^{\#\#}P < 0.01$; $^{\#\#\#}P < 0.001$ vs L+H; 1-way ANOVA and Tukey post hoc tests. Abbreviations as in Figures 1, 4, and 5.

proinflammatory cells around lymphatic vessels.[34] However, there was no direct evidence that impairment of the lymphatic system is a positive driver of HFpEF development. One study demonstrated that cardiac lymphatic obstruction could induce depressed contractility, relaxation, and mild left ventricular myocardial edema, but did not alter diastolic stiffness or morphologic changes in a short period.[30] In the present study, however, we could observe the HFpEF condition with cardiac morphologic changes such as fibrosis, inflammatory cell infiltration, and interstitial edema. Our results revealed that lymphatic dysfunction could lead to cardiac diastolic dysfunction via inducing the accumulation of inflammatory cells, fibrotic change, and hypertrophy resulting from the up-regulation of local inflammatory cytokines (TNF-α, IL-1β, and IL-6), profibrotic molecules (COL1A1, TGF-β, and Postn), and hypertrophic signaling molecules (β-MHC, TRPC6, RCAN-1, and CT-1) under both physiologic and pathologic conditions. It has been reported that cell therapy, including ADRC implantation, exerts anti-inflammatory effects in pathologic conditions, which itself is one of the mechanisms that contribute to tissue repair and organ protection. For example, ADRCs secrete prostaglandin E2 and switch the polarity of local macrophages from proinflammatory (M1 type) to anti-inflammatory (M2 type).[35] Here, the therapeutic lymphangiogenesis by ADRCs was shown to promote the drainage of inflammatory cells, thereby indirectly ameliorating inflammation. Importantly, therapeutic lymphangiogenesis with ADRC implantation could ameliorate these pathologic responses and restore cardiac function.

STUDY LIMITATIONS. There are several limitations in this study. Primarily, left ventricular end-diastolic pressure and exercise capacity in animals with lymph ablations were not evaluated owing to the lack of systems doing so in our laboratory. These both represent important physiologic determinants of HFpEF. A future study to evaluate these parameters would be warranted.

CONCLUSIONS

We established a first-ever mouse model of cardiac lymphatic dysfunction and demonstrated the crucial role of cardiac lymphatic vessels in maintaining cardiac homeostasis and diastolic function in both physiologic and pathologic settings (Supplemental Figure 4). These findings suggest that modulation of the cardiac lymphatic system would be a novel therapeutic target for HFpEF patients in the future.

ACKNOWLEDGMENTS The authors are grateful to the staff from the Division of Experimental Animals at the Nagoya University School of Medicine for assisting with animal experiments. They thank Ms. Yoko Inoue for her technical assistance.

FUNDING SUPPORT AND AUTHOR DISCLOSURES

This work was supported by Ministry of Education, Culture, Sports, Science and Technology of Japan grant 19K17519 (Dr Shimizu) and a Chukyo Longevity Medical and Promotion Foundation grant (Dr Shimizu.). The authors have reported that they have no relationships relevant to the contents of this paper to disclose.

ADDRESS FOR CORRESPONDENCE: Dr Yuuki Shimizu, Department of Cardiology, Nagoya University Graduate School of Medicine, 65 Tsurumai, Showa-ku, Nagoya 466-8550, Japan. E-mail: shimi123@med.nagoya-u.ac.jp.

PERSPECTIVES

COMPETENCY IN MEDICAL KNOWLEDGE: For the terminal stage of clinical heart failure, cardiac transplantation is one of the last available therapeutic strategies. Although heart transplantation involves complete vascular reconstruction, the reconstruction of cardiac nerves and lymphatic vessels is not considered. It therefore remains unclear whether the disruption of nerves and lymphatic vessels affects both systolic and diastolic function of the transplanted heart and the eventual engraftment rate. After heart transplantation, immunologic rejection, inflammation, and fibrosis are very important issues in terms of not only the engraftment rate, but also functional maintenance. In this study, we found that disruption of the cardiac collecting lymphatics even in the normal heart could induce inflammation and edema, resulting in myocardial hypertrophy and diastolic dysfunction. In addition, promoting lymphangiogenesis could alleviate these adverse changes and lead to cardioprotection. Taken together, the management of cardiac lymphatic vessels in heart transplantation might be an important additional strategy to improve outcomes.

TRANSLATIONAL OUTLOOK: At present, therapeutic options are still limited for patients with HFpEF. A very recent clinical study showed that a sodium-glucose cotransporter 2 inhibitor, empagliflozin, can reduce heart failure events in HFpEF patients (the EMPEROR-Preserved trial).[36] However, the precise therapeutic mechanism of this SGLT2 inhibitor remains largely unclear. The present study clearly suggests that cardiac lymphatic insufficiency contributes to the development of myocardial edema, inflammation, hypertrophy, and HFpEF status. Therefore, future research to elucidate the potential effects of therapeutic lymphangiogenesis on HFpEF conditions is warranted.

REFERENCES

1. Makinen T, Boon LM, Vikkula M, Alitalo K. Lymphatic malformations: genetics, mechanisms and therapeutic strategies. *Circ Res*. 2021;129:136–154.

2. Karkkainen MJ, Alitalo K. Lymphatic endothelial regulation, lymphoedema, and lymph node metastasis. *Semin Cell Dev Biol*. 2002;13:9–18.

3. Vaahtomeri K, Karaman S, Makinen T, Alitalo K. Lymphangiogenesis guidance by paracrine and pericellular factors. *Genes Dev*. 2017;31:1615–1634.

4. Zheng W, Aspelund A, Alitalo K. Lymphangiogenic factors, mechanisms, and applications. *J Clin Invest*. 2014;124:878–887.

5. Karkkainen MJ, Haiko P, Sainio K, et al. Vascular endothelial growth factor C is required for sprouting of the first lymphatic vessels from embryonic veins. *Nat Immunol*. 2004;5:74–80.

6. Klotz L, Norman S, Vieira JM, et al. Cardiac lymphatics are heterogeneous in origin and respond to injury. *Nature*. 2015;522:62–67.

7. Choi I, Lee S, Kyoung Chung H, et al. 9-Cis retinoic acid promotes lymphangiogenesis and enhances lymphatic vessel regeneration: therapeutic implications of 9-cis retinoic acid for secondary lymphedema. *Circulation*. 2012;125:872–882.

8. Shimizu Y, Polavarapu R, Eskla KL, et al. Impact of lymphangiogenesis on cardiac remodeling after ischemia and reperfusion injury. *J Am Heart Assoc*. 2018;7:e009565.

9. Brakenhielm E, Alitalo K. Cardiac lymphatics in health and disease. *Nat Rev Cardiol*. 2019;16:56–68.

10. Pu Z, Shimizu Y, Tsuzuki K, et al. Important role of concomitant lymphangiogenesis for reparative angiogenesis in hindlimb ischemia. *Arterioscler Thromb Vasc Biol*. 2021;41:2006–2018.

11. Shimizu Y, Nicholson CK, Polavarapu R, et al. Role of DJ-1 in modulating glycative stress in heart failure. *J Am Heart Assoc*. 2020;9:e014691.

12. Tsuzuki K, Shimizu Y, Suzuki J, et al. Adverse effect of circadian rhythm disorder on reparative angiogenesis in hind limb ischemia. *J Am Heart Assoc*. 2021;10:e020896.

13. Murphy E, Lagranha C, Deschamps A, et al. Mechanism of cardioprotection: what can we learn from females? *Pediatr Cardiol*. 2011;32:354–359.

14. Suzuki J, Shimizu Y, Tsuzuki K, et al. No influence on tumor growth by intramuscular injection of adipose-derived regenerative cells: safety evaluation of therapeutic angiogenesis with cell therapy. *Am J Physiol Heart Circ Physiol*. 2021;320:H447–H457.

15. Shimizu Y, Shibata R, Shintani S, Ishii M, Murohara T. Therapeutic lymphangiogenesis with implantation of adipose-derived regenerative cells. *J Am Heart Assoc*. 2012;1:e000877.

16. Barr LA, Shimizu Y, Lambert JP, Nicholson CK, Calvert JW. Hydrogen sulfide attenuates high fat diet-induced cardiac dysfunction via the suppression of endoplasmic reticulum stress. *Nitric Oxide*. 2015;46:145–156.

17. Shimizu Y, Nicholson CK, Lambert JP, et al. Sodium sulfide attenuates ischemic-induced heart failure by enhancing proteasomal function in an Nrf2-dependent manner. *Circ Heart Fail*. 2016;9:e002368.

18. Shimizu Y, Shibata R, Ishii M, et al. Adiponectin-mediated modulation of lymphatic vessel formation and lymphedema. *J Am Heart Assoc*. 2013;2:e000438.

19. Alitalo K, Tammela T, Petrova TV. Lymphangiogenesis in development and human disease. *Nature*. 2005;438:946–953.

20. Petrova TV, Koh GY. Organ-specific lymphatic vasculature: from development to pathophysiology. *J Exp Med*. 2018;215:35–49.

21. Cui Y. The role of lymphatic vessels in the heart. *Pathophysiology*. 2010;17:307–314.

22. Fudim M, Salah HM, Sathananthan J, et al. Lymphatic dysregulation in patients with heart failure: JACC review topic of the week. *J Am Coll Cardiol*. 2021;78:66–76.

23. Henri O, Pouehe C, Houssari M, et al. Selective stimulation of cardiac lymphangiogenesis reduces myocardial edema and fibrosis leading to improved cardiac function following myocardial infarction. *Circulation*. 2016;133:1484–1497. discussion 1497.

24. Ishikawa Y, Akishima-Fukasawa Y, Ito K, et al. Lymphangiogenesis in myocardial remodelling after infarction. *Histopathology*. 2007;51:345–353.

25. Kholova I, Dragneva G, Cermakova P, et al. Lymphatic vasculature is increased in heart valves, ischaemic and inflamed hearts and in cholesterol-rich and calcified atherosclerotic lesions. *Eur J Clin Invest*. 2011;41:487–497.

26. Kline IK, Miller AJ, Pick R, Katz LN. The relationship between human endocardial fibroelastosis and obstruction of the cardiac lymphatics. *Circulation*. 1964;30:728–735.

27. Dongaonkar RM, Stewart RH, Geissler HJ, Laine GA. Myocardial microvascular permeability, interstitial oedema, and compromised cardiac function. *Cardiovasc Res*. 2010;87:331–339.

28. Laine GA, Allen SJ. Left ventricular myocardial edema. Lymph flow, interstitial fibrosis, and cardiac function. *Circ Res*. 1991;68:1713–1721.

29. Kline IK, Miller AJ, Katz LN. Cardiac lymph flow impairment and myocardial fibrosis. effects of chronic obstruction in dogs. *Arch Pathol*. 1963;76:424–433.

30. Ludwig LL, Schertel ER, Pratt JW, et al. Impairment of left ventricular function by acute cardiac lymphatic obstruction. *Cardiovasc Res*. 1997;33:164–171.

31. Wang YL, Wang XH, Liu YL, Kong XQ, Wang LX. Cardiac lymphatic obstruction impairs left ventricular function and increases plasma endothelin-1 and angiotensin II in rabbits. *Lymphology*. 2009;42:182–187.

32. Zawieja SD, Wang W, Chakraborty S, Zawieja DC, Muthuchamy M. Macrophage alterations within the mesenteric lymphatic tissue are associated with impairment of lymphatic pump in metabolic syndrome. *Microcirculation*. 2016;23:558–570.

33. Liao S, Cheng G, Conner DA, et al. Impaired lymphatic contraction associated with immunosuppression. *Proc Natl Acad Sci U S A*. 2011;108:18784–18789.

34. Nitti MD, Hespe GE, Kataru RP, et al. Obesity-induced lymphatic dysfunction is reversible with weight loss. *J Physiol*. 2016;594:7073–7087.

35. Hao C, Shintani S, Shimizu Y, et al. Therapeutic angiogenesis by autologous adipose-derived regenerative cells: comparison with bone marrow mononuclear cells. *Am J Physiol Heart Circ Physiol*. 2014;307:H869–H879.

36. Anker SD, Butler J, Filippatos G, et al. Empagliflozin in Heart failure with a preserved ejection fraction. *N Engl J Med*. 2021;385:1451–1461.

KEY WORDS cardiac diastolic dysfunction, cardiac lymphatic vessels, fibrosis, hypertrophy, inflammation

APPENDIX For a supplemental Methods section, and supplemental figures, please see the online version of this paper.